Scattering of massless fermions by Schwarzschild and Reissner-Nordström black holes[*]

Ciprian A. Sporea[1)]

West University of Timişoara, V. Pârvan Ave. 4, RO-300223 Timişoara, Romania

Abstract: We study the scattering of massless Dirac fermions by Schwarzschild and Reissner-Nordström black holes. This is done by applying partial wave analysis to the scattering modes obtained after solving the massless Dirac equation in the asymptotic regions of the two black hole geometries. We successfully obtain analytic phase shifts, with the help of which the scattering cross section is computed. The glory and spiral scattering phenomena are shown to be present, as in the case of massive fermion scattering by black holes.

1 Introduction

The problem of black hole scattering is still ongoing, despite the numerous papers that have dealt with it so far. Most of these studies have been dedicated to investigating different aspects of (massless) scalar wave scattering by black holes [1–23]. However, there are also papers that study the scattering of massless electromagnetic waves [24–32] and gravitational waves [33–40]. The problem of scattering of massive spinor 1/2 waves by black holes was discussed in Refs. [5, 41–50]. The scattering of massless fermions was studied in Refs. [51, 52], where the scattering of massless fermions by a black hole with a cosmic string and by a dilatonic black hole, respectively, was investigated. It was also partially investigated in Ref. [46] for a Schwarzschild black hole. The authors of Ref. [46] used numerical methods to solve the Dirac equation in Schwarzschild black hole geometries in order to find numerical phase shifts using a partial wave analysis. In Ref. [49] we obtained, for the first time, analytic expressions for the Schwarzschild phase shifts. Furthermore, in Ref. [50] we extended our study to include the case of fermion scattering by charged Reissner-Nordström black holes, where we again found analytic phase shifts. Moreover, our study in Ref. [50] is to our knowledge the first in the literature in which the problem of massive fermion scattering by Reissner-Nordström black holes was investigated.

In this paper we study the scattering of massless fermions by spherical symmetric black holes, with a focus on Schwarzschild and charged Reissner-Nordström black holes. We derive analytic phase shifts that will allow us to write down analytic expressions for the scattering cross sections.

Although it is generally assumed that astrophysical black holes are electrically neutral [53], or at least have negligible charges, it has been recently shown in Ref. [54] that charged astrophysical black holes can in fact exist in the context of minicharged dark matter models [55]. These dark matter models predict new fermions that can have fractional electric charge or fermions that are charged under a $U(1)$ hidden symmetry. Because these new charges have just a small fraction of the electron's charge, their coupling with the Standard Model electromagnetic sector is suppressed. This means that even in the case of massive fermions there could be no direct interaction between the Dirac field and the electromagnetic field of the black hole. This could open new possibilities for dark matter detection through neutrino-wave scattering by black holes, besides the gravitational-wave signatures discussed in Ref. [56].

In the original Standard Model of particle physics neutrinos are assumed to be massless. Therefore, our results will include the case of massless neutrino scattering by black holes (see also Appendix A). However, it has been observed experimentally [57, 58] that neutrinos have a nonzero mass that it is currently bound to $\sum m_\nu < 0.183$ eV [59]. The electron neutrino mass could be as small as $m_{\nu_e} \sim 0.01$ eV or smaller. Having this in mind one can easily assume that our results (presented in the following sections) will give also a good approximation for the cross sections in the case of scattering of

astrophysical neutrinos by black holes.

The paper is organised as follows. In Section 2 we give a brief introduction of the general form of the massless Dirac equation in a curved spacetime with spherical symmetry. The Cartesian gauge is introduced and the separation of spherical variables is made. In the Section 3 we solve the massless Dirac equation in the case of Schwarzschild and Reissner-Nordström black hole geometries. We focus only on scattering mode solutions. Section 4 deals with the partial wave analysis, where we give analytical expressions for the phase shifts that enter into the definitions of the scattering amplitudes and cross sections. Section 5 presents the main results obtained. The paper ends with Section 6, where the final conclusions and some remarks are presented.

In this paper we set $G=c=\hbar=1$; the metric signature used is $(+,-,-,-)$; and the natural indices are labeled with Greek letters $\mu,\nu,\alpha,...$, while the local indices are labeled with $a,b,c,...$; both can take values in the range $(0,1,2,3)$.

2   Preliminaries

Starting from the gauge invariant action

$$\mathcal{S}=\int \mathrm{d}^4x \ \sqrt{-g}\left\{\frac{\mathrm{i}}{2}\overline{\psi}\gamma^a D_a\psi-\frac{\mathrm{i}}{2}(\overline{D_a\psi})\gamma^a\psi\right\}, \quad (1)$$

we can immediately derive the following Dirac equation for a massless spinor field in a curved spacetime

$$\mathrm{i}\gamma^a e_a^\mu\partial_\mu\psi+\frac{\mathrm{i}}{2}\frac{1}{\sqrt{-g}}\partial_\mu(\sqrt{-g}e_a^\mu)\gamma^a\psi-\frac{1}{4}\{\gamma^a,S_c^b\}\omega_{ab}^c\psi=0, \quad (2)$$

where e_a^μ are the tetrad fields such that $g^{\mu\nu}=\eta^{ab}e_a^\mu e_b^\nu$; γ^a are the point-independent Dirac matrices satisfying $\{\gamma^a,\gamma^b\}=2\eta^{ab}$; and S_c^b are the generators of the spinor representation of $SL(2,\mathbb{C})$ [60] such that $S^{ab}=\frac{\mathrm{i}}{4}[\gamma^a,\gamma^b]$;

The covariant derivative D_a and the spin-connection read

$$D_a=\partial_a+\frac{\mathrm{i}}{2}S_c^b\omega_{ab}^c$$
$$\omega_{ab}^c=e_a^\mu e_b^\nu\left(\hat{e}_\lambda^c\Gamma_{\mu\nu}^\lambda-\hat{e}_{\nu,\mu}^c\right) \quad (3)$$

with $\partial_a=e_a^\mu\partial_\mu$ and $\Gamma_{\mu\nu}^\lambda$ stand for the GR Christoffel symbols.

The spacetime geometry of a spherically symmetric black hole is given by the following line element

$$\mathrm{d}s^2=h(r)\mathrm{d}t^2-\frac{\mathrm{d}r^2}{h(r)}-r^2\left(\mathrm{d}\theta^2+\sin^2\theta\mathrm{d}\phi^2\right). \quad (4)$$

In the Cartesian gauge [62, 63], the above line element can be obtained from $\mathrm{d}s^2=\eta_{ab}\hat{e}^a\hat{e}^b$ with the following choice of the tetrad field $\hat{e}^a(x)=\hat{e}_\mu^a\mathrm{d}x^\mu$ (i.e. the 1-forms)

$$\hat{e}^0=h(r)\mathrm{d}t,$$
$$\hat{e}^1=\frac{1}{h(r)}\sin\theta\cos\phi\mathrm{d}r+r\cos\theta\cos\phi\mathrm{d}\theta-r\sin\theta\sin\phi\mathrm{d}\phi,$$
$$\hat{e}^2=\frac{1}{h(r)}\sin\theta\sin\phi\mathrm{d}r+r\cos\theta\sin\phi\mathrm{d}\theta+r\sin\theta\cos\phi\mathrm{d}\phi,$$
$$\hat{e}^3=\frac{1}{h(r)}\cos\theta\mathrm{d}r-r\sin\theta\mathrm{d}\theta. \quad (5)$$

The main advantage of the above Cartesian gauge is that in this gauge the Dirac equation (free or in central scalar potentials) is manifestly covariant under rotations. This means that the angular part of the equation can be solved in terms of the usual 4-component angular spinors from special relativity $\Phi_{m,\kappa}^\pm(\theta,\phi)$ [60, 61]. Using the Cartesian gauge, new (exact or approximate) analytical solutions of the Dirac equation in curved backgrounds were found [68–71].

Inserting the metric (4) in Eq. (2) and after some calculations, one can put the Dirac equation into a Hamiltonian form $H\psi(x)=\mathrm{i}\partial_t\psi(x)$, with

$$H_D=-\mathrm{i}\gamma^0(\vec{\gamma}\cdot\vec{e}_r)\left(h\partial_r+\frac{h}{r}-\frac{\sqrt{h}}{r}K\right) \quad (6)$$

and where $K=2\vec{S}\cdot\vec{L}+1=J^2-L^2+\frac{1}{4}$ is the spin-orbit operator [60], whose eigenvalues κ are related those of the total angular momentum operator (J) and of the orbital angular momentum (L) by

$$\kappa=\begin{cases} -\left(j+\dfrac{1}{2}\right)=-(l+1) & \text{for} \quad j=l+\dfrac{1}{2} \\ +\left(j+\dfrac{1}{2}\right)=l & \text{for} \quad j=l-\dfrac{1}{2} \end{cases}. \quad (7)$$

The radial part of the Dirac equation can be derived by searching for (particle-like) positive frequency solutions of energy E of the type

$$\psi(x)=\psi_{E,\kappa,m_j}(t,r,\theta,\phi)=$$
$$=\frac{\mathrm{e}^{-\mathrm{i}Et}}{r\sqrt{h(r)}}\left\{f_{E,\kappa}^+(r)\Phi_{m_j,\kappa}^+(\theta,\phi)+f_{E,\kappa}^-(r)\Phi_{m_j,\kappa}^-(\theta,\phi)\right\}. \quad (8)$$

One can show that the final form of the equations satisfied by the radial wave-functions $f^\pm(r)$ (where for simplicity we have dropped the indices E and κ) is

$$\begin{pmatrix} 0 & -h(r)\dfrac{\mathrm{d}}{\mathrm{d}r}+\dfrac{\kappa}{r}\sqrt{h(r)} \\ h(r)\dfrac{\mathrm{d}}{\mathrm{d}r}+\dfrac{\kappa}{r}\sqrt{h(r)} & 0 \end{pmatrix}\begin{pmatrix} f^+(r) \\ f^-(r) \end{pmatrix}=E\begin{pmatrix} f^+(r) \\ f^-(r) \end{pmatrix}. \quad (9)$$

3　Massless Dirac equation in Schwarzschild and Reissner-Nordström geometry

As already mentioned in the Introduction, we are studying here only the scattering of massless fermions by black holes. For that we need first to find the scattering modes of the Dirac equation (9) on which to apply the partial wave analysis (PWA) method. That will allow us to find the phase shifts and then to calculate all the physical quantities that are characteristic of the scattering phenomena. For PWA one only needs to know the asymptotic behaviour of the scattering modes. As shown below, in the asymptotic region of both the Schwarzschild and RN black hole, the Dirac equation (9) can be brought to a simpler form that will allow us to solve it analytically. Furthermore, having an analytical solution at our disposal will allow us to find analytical phase shifts.

In the case of a Reissner-Nordström black hole, the function $h(r)$ entering the line element (4) is defined by

$$h(r)=1-\frac{2M}{r}+\frac{Q^2}{r^2}=\left(1-\frac{r_+}{r}\right)\left(1-\frac{r_-}{r}\right), \qquad (10)$$

where M is the mass of the black hole and Q the electric charge. The Cauchy (r_-) and black hole horizon (r_+) radii are easily found to be $r_\pm=M\pm\sqrt{M^2-Q^2}$ (provided $Q<M$). If we make $Q=0$ in Eq. (10) we obtain the Schwarzschild line element with $r_-=r_+=r_0=2M$.

It proves useful to introduce a convenient Novikov-like dimensionless coordinate [65, 66]

$$x=\sqrt{\frac{r}{r_+}-1}\in(0,\infty). \qquad (11)$$

Then the Dirac equation (9) in the asymptotic region of the black hole becomes

$$\begin{pmatrix} \frac{1}{2}\frac{\mathrm{d}}{\mathrm{d}x}+\frac{\kappa}{x} & -\varepsilon\left(x+\frac{1}{x}\right) \\ \varepsilon\left(x+\frac{1}{x}\right) & \frac{1}{2}\frac{\mathrm{d}}{\mathrm{d}x}-\frac{\kappa}{x} \end{pmatrix}\begin{pmatrix} f^+(x) \\ f^-(x) \end{pmatrix}=0, \qquad (12)$$

where we denoted $\varepsilon=r_+E$. In obtaining Eq. (12) we have used a Taylor expansion with respect to $1/x$, from which we neglected the $O(1/x^2)$ terms and higher.

After putting the terms proportional with x into diagonal form, using the transformation matrix

$$M=\sqrt{\varepsilon}\begin{pmatrix} -\mathrm{i} & \mathrm{i} \\ 1 & 1 \end{pmatrix}, \qquad (13)$$

that transforms $(f^+,f^-)^T\to(\hat{f}^+,\hat{f}^-)^T=M^{-1}(f^+,f^-)^T$, the final system of radial equations is obtained

$$\frac{1}{2}\frac{\mathrm{d}\hat{f}^+}{\mathrm{d}x}-\mathrm{i}\varepsilon\left(x+\frac{1}{x}\right)\hat{f}^+=\frac{\kappa}{x}\hat{f}^-$$

$$\frac{1}{2}\frac{\mathrm{d}\hat{f}^-}{\mathrm{d}x}+\mathrm{i}\varepsilon\left(x+\frac{1}{x}\right)\hat{f}^-=\frac{\kappa}{x}\hat{f}^+. \qquad (14)$$

The analytical solutions of the above equations can be found in terms of Whittaker M and W functions [49, 50, 71]

$$\hat{f}^+(x)=C_1\frac{1}{x}M_{\rho_+,s}(2\mathrm{i}\varepsilon x^2)+C_2\frac{1}{x}W_{\rho_+,s}(2\mathrm{i}\varepsilon x^2)$$

$$\hat{f}^-(x)=C_1\frac{s-\mathrm{i}\varepsilon}{\kappa}\frac{1}{x}M_{\rho_-,s}(2\mathrm{i}\varepsilon x^2)-C_2\frac{1}{\kappa}\frac{1}{x}W_{\rho_-,s}(2\mathrm{i}\varepsilon x^2), \qquad (15)$$

where the parameters $s,\rho_\pm$ are related to κ and ε by the following relations

$$s=\sqrt{\kappa^2-\varepsilon^2}, \quad \rho_\pm=\mp\frac{1}{2}-\mathrm{i}\varepsilon. \qquad (16)$$

These solutions are the starting point for studying the scattering phenomena by Schwarzschild and Reissner-Nordström black holes with the help of partial wave analysis. The Whittaker functions $M_{\rho_\pm,s}(2\mathrm{i}\varepsilon x^2)=(2\mathrm{i}\varepsilon x^2)^{s+\frac{1}{2}}[1+O(x^2)]$ are regular in $x=0$ (i.e. in $r=r_+$), while the Whittaker $W_{\rho_\pm,s}(2\mathrm{i}\varepsilon x^2)$ are divergent as x^{1-2s} if $s>\frac{1}{2}$ [67]. As showed in the Appendices of Refs. [49] and [50] one must impose the asymptotic condition $C_2=0$ in order to have elastic collisions with a correct Newtonian limit for large angular momentum.

4　Scattering cross section and phase shifts

The phase shifts that result after applying the partial wave analysis [49, 50] on the scattering modes (15) are defined by

$$S_\kappa=\mathrm{e}^{2\mathrm{i}\delta_\kappa}=\left(\frac{\kappa}{s-\mathrm{i}\varepsilon}\right)\frac{\Gamma(1+s-\mathrm{i}\varepsilon)}{\Gamma(1+s+\mathrm{i}\varepsilon)}\mathrm{e}^{\mathrm{i}\pi(l-s)}. \qquad (17)$$

The scattering amplitudes are defined by [61]

$$f(\theta)=\sum_{l=0}^{\infty}a_lP_l(\cos\theta), \quad g(\theta)=\sum_{l=1}^{\infty}b_lP_l^1(\cos\theta), \qquad (18)$$

where a_l and b_l are the partial amplitudes

$$a_l=\frac{1}{2\mathrm{i}p}[(l+1)(S_{-l-1}-1)+l(S_l-1)]$$

$$b_l=\frac{1}{2\mathrm{i}p}(S_{-l-1}-S_l). \qquad (19)$$

Putting all together one gets the differential scattering cross section

$$\frac{\mathrm{d}\sigma}{\mathrm{d}\Omega}=|f(\theta)|^2+|g(\theta)|^2. \qquad (20)$$

In the next section we will give a selection of our key results for the scattering of massless fermions by Schwarzschild and Reissner-Nordström black holes. In the derivation of the plots we have used a method first proposed in Ref. [64] and further developed in Refs. [46, 49, 50] for improving the convergence of the partial wave series (18).

5   Results

In Fig. 1 we compare the scattering of massless ($v=1$) and massive ($v \neq 1$) fermions by a Schwarzschild black hole ($q=0$) for a fixed value of the (frequency) parameter ME. The case of massive fermion scattering by Schwarzschild and Reissner-Nordström black holes was studied in more detail in our previous papers [49, 50]. Analyzing the differential cross section in the backward direction (near $\theta \approx \pi$) one can see a minimum in the scattering intensity. If the fermion is massive then the scattering intensity in the backward direction is higher than in the massless case. Moreover, with decreasing fermion speed, the minimum will eventually become a maximum in the backward direction (see Ref. [49] for more details).
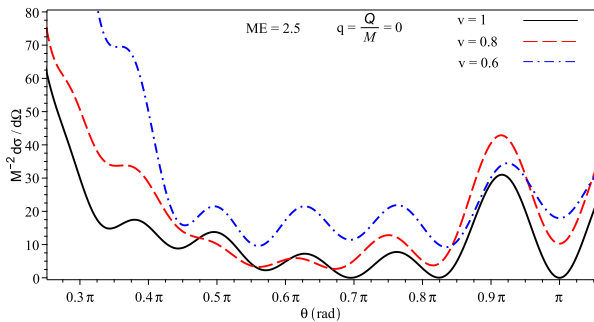

Fig. 1. (color online) Comparison between the scattering of massless ($v=1$) and massive ($v \neq 1$) fermions by a Schwarzschild black hole at $ME = 2.5$. The presence of a minimum in the backward direction can be observed.

In optics the presence of a minimum or maximum in the scattering intensity in the backward direction occurs when the deflection angle of a ray is a multiple of π. This is observed by the presence of a bright spot or halo in the antipodal direction. If the orbit passes the scattering center multiple times, then spiral (or orbiting) scattering can occur. This can be seen by the presence of oscillations in the scattering intensity. As can be seen from Figs. 1-5, the phenomena of glory and spiral scattering also occur in the case of massless fermion scattering by Schwarzschild and charged Reissner-Nordström black holes.

In Fig. 2 we plot the scattering intensity for a massless spinor wave of fixed frequency for a Schwarzschild black hole ($q=0$), a typical Reissner-Nordström black hole (with $q=0.5, q=0.6, q=0.9$), and an extremal Reissner-Nordström black hole ($q=1$). One can observe (very clearly for $ME=3$) that at a fixed frequency the glory width gets larger as the value of the charge-to-mass ratio q increases. The same behaviour was also reported in Ref. [17] in the case of scattering of massless scalar waves by Reissner-Nordström black holes. In Ref. [51] the authors found that the linear mass density of the cos-

mic string produces a similar effect. Furthermore, the oscillations present in the scattering intensity become less frequent as we approach the extremal case $q=1$. This means that the spiral scattering becomes less important as the black hole gets more and more charge on it.
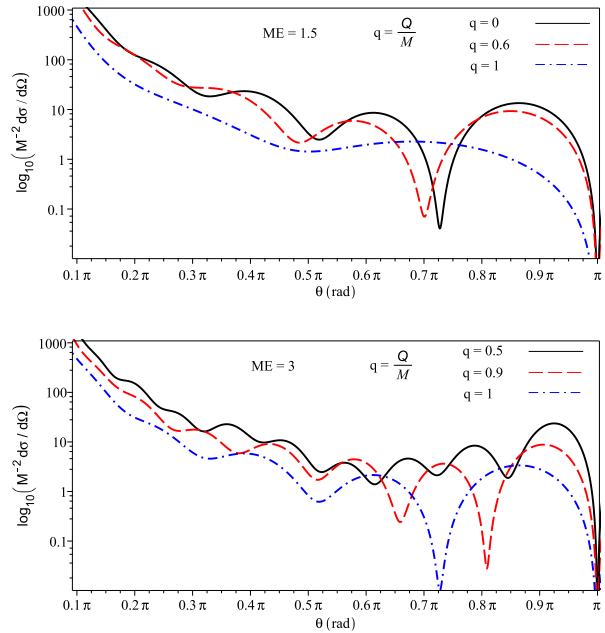

Fig. 2. (color online) Comparison between the massless fermion scattering cross section at fixed frequency $ME=1.5$ for $q=0, q=0.6$, $q=1$ in one case and at $ME=3$ for $q=0.5, q=0.9$, $q=1$ in the other case. Fixing the frequency, the glory width gets larger as the value of the charge-to-mass ratio q increases.

In Fig. 3 the differential scattering cross section for the massless fermion field is plotted, using a logarithmic scale, for different values of the incoming fermion frequency $ME = 2.5, 3, 3.5$ at a chosen fixed value of the charge-to-mass ratio $q = 0$ (Schwarzschild case), $q=0.5$ (typical Reissner-Nordström) and $q=1$ (extremal Reissner-Nordström case). The first thing to observe is that the width of the glory becomes narrower as the frequency increases. The oscillations (indicating spiral scattering) present in the scattering intensity become more frequent, however, as the value of ME is increased. This can be best seen for the extremal case $q=1$.

Figure 4 shows the behaviour of the massless fermion differential scattering cross section at low frequency for a typical Reissner-Nordström black hole ($q=0.5$). In Fig. 5 the extremal Reissner-Nordström case ($q=1$) is studied for a large variance of ME. We notice the absence of oscillations at very low frequency ($ME=0.1$) in the differential scattering cross section. However, as the value of ME is increased, the spiral scattering and eventually glory start to occur.
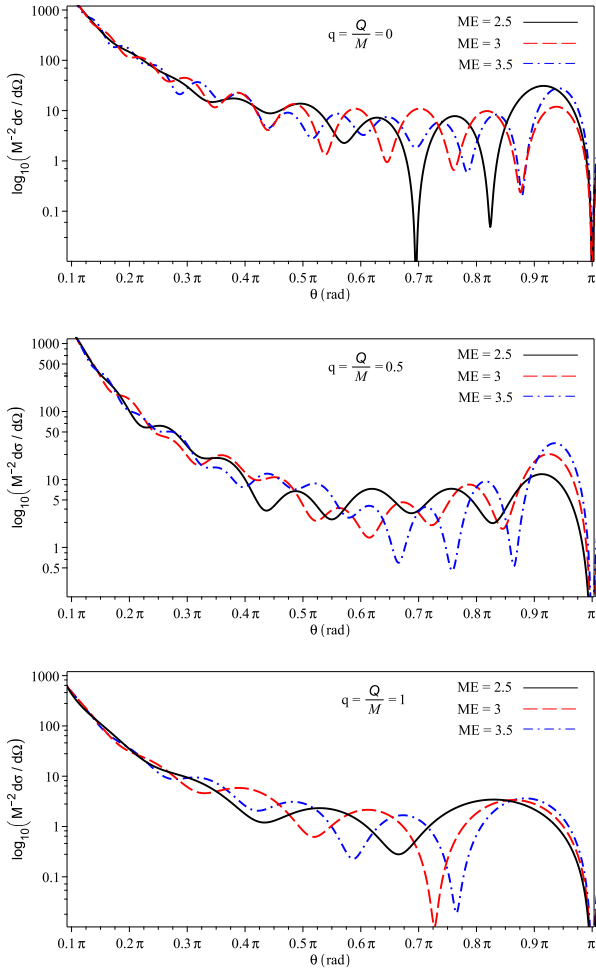
Fig. 3.   (color online) Reissner-Nordström scatter-
ing intensity for $ME = 2.5$, 3, 3.5 in the case of
a black hole with no charge $q = 0$, with charge
$q = 0.5$ and the extremal case with charge $q = 1$.
Increasing the frequency causes narrowing of the
glory width. At the same time, the oscillations in
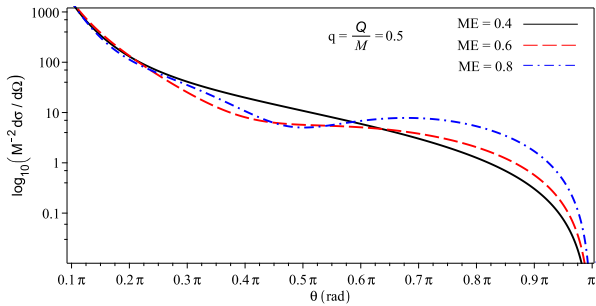the scattering intensity become more frequent.

Fig. 4.   (color online) Differential scattering cross
section for massless fermions at low frequen-
cies ($ME = 0.4, 0.6, 0.8$) for a typical Reissner-
Nordström black hole with charge $q=0.5$.

Exploring the parameter space (q, ME), we have
found situations when two different sets of parameters

present similar scattering patterns (see Fig. 6). In some
cases (like in Fig. 6B) the scattering patterns are almost
the same. For example, the difference between the val-
ues in the scattering intensity of $(0.6, 1.1)$ and $(1.0, 0.2)$
curves is less than 17%. As a consequence, one will need
higher accuracy in the observed data in order to distin-
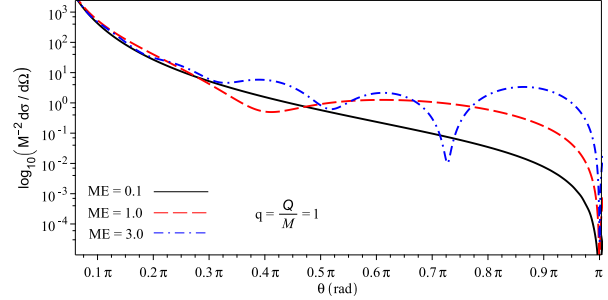guish between the two data sets.

Fig. 5.   (color online) Scattering cross section for
extremal Reissner-Nordström black hole ($q = 1$)
for $ME = 0.1, 1, 3$. Increasing the value of ME,
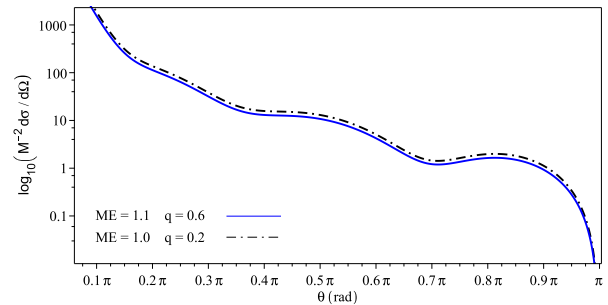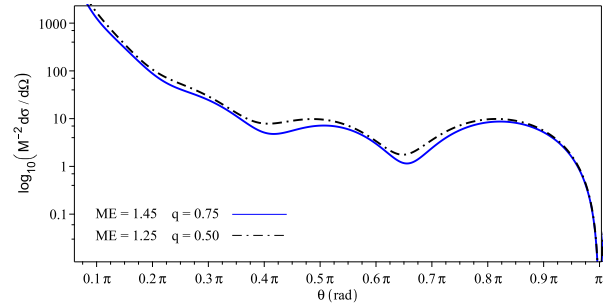spiral scattering and glory start to occur in the
scattering intensity.

Fig. 6.   (color online) Dependence of the scattering
pattern on the black hole charge and frequency.
One can observe similarities between the scatter-
ing patterns for certain values in the parameter
space (q, ME).

6   Conclusions and final remarks

In this paper we have studied the scattering of mass-
less fermions by Schwarzschild and charged Reissner-
Nordström black holes. We have showed that glory and

spiral scattering phenomena could occur for both types of black holes analysed, similar to what happens in the case of massive fermion scattering by black holes [46, 49, 50]. As can be seen from Figs. 1–5, the scattering of massless fermions always has a minimum in the backward direction (as opposed to the massless scalar case [17]). However, if the fermion becomes massive (see Fig. 1), then this minimum starts to increase and will become eventually a maximum [49].

The dependence of the scattering on the charge-to-mass ratio $q = Q/M$ was analysed for typical values including the extreme case $q = 1$. As shown in Fig. 2, for a fixed value of ME the glory width gets larger as the value of q is increased. One the other hand, keeping the value of q fixed and varying the frequency ME we observe an increase in the number of oscillations present in the scattering intensity, as shown in Fig. 3.

As already mentioned, at a fixed frequency, the glory pick is wider in the case of the Reissner-Nordström black hole ($q \neq 0$) compared with the Schwarzschild black hole ($q = 0$). As a consequence the glory phenomenom will be easier to observe astronomically for a Schwarzschild black hole than for a charged Reissner-Nordström one. Moreover, the glory for the extremal Reissner-Nordström case is the hardest for astronomy observation.

We have used the parameter ME to label our figures. Restoring the units we can make the following dimensionless quantity

$$\epsilon = \frac{GME}{\hbar c^3} = \frac{\pi r_S}{v \lambda_C}, \qquad (21)$$

where $r_S = 2MG$ is the Schwarzschild gravitational radius, $\lambda_C = h/p$ is the associated Compton wavelength of the particle and $v = p/E$ is its speed ($v = 1$ for massless fermions). One can interpret ϵ as a measure of the gravitational coupling. The results obtained in the previous sections show that glory and spiral scattering of massless fermions by black holes are significant when the gravitational coupling is of the order of π. This implies that

we must have $r_S \sim \lambda_C$. Thus we can conclude that the diffraction patterns of massless fermions (like the glory and spiral scattering) by black holes are significant if the condition $r_S \sim \lambda_C$ is fulfilled.

Neutrinos have the smallest mass of the fermions known experimentally today. The current upper bound limit on the sum of the three known neutrinos is $\sum m_\nu < 0.183 eV$ [59]. If we assume the mass of the electron neutrino to be $m_{\nu_e} \sim 0.01 eV$, then the condition $r_S \sim \lambda_C$ implies a black hole mass of $M \sim 10^{22}$ kg, which is much smaller than the mass of an astrophysical stelar black hole $M_{BH} \sim 10^{31}$ kg. This means that neutrino glory and spiral scattering can be observed only for scattering by small black holes. Such types of primordial black holes could have been created in the very early universe. Another possible scenario for the existence of such small black holes is in the context of theories with large extra-dimensions [72]. In these circumstances the possibilities of observing and detecting diffraction patterns for massive fermion scattering by black holes are currently unavailable. However, in the case of the existence of truly massless fermions (yet to be detected) we are no longer bound by the mass of the fermion (which as we saw constrains also the possible mass of the black hole), which means that glory and spiral scattering can in principle be observed for the scattering of massless fermions (having appropriate energies) by real astrophysical black holes.

Appendix A

Neutrino limit to the Dirac field

The aim of this Appendix is to show that the scattering of the Standard Model neutrino (which is a left-handed massless Dirac fermion) by black holes is contained in our results presented here regarding the scattering of massless Dirac fermions.

The following combination of the (f_κ^+, f_κ^-) radial wave functions

$$f_\kappa^L = \frac{1}{\sqrt{2}} \left(f_\kappa^+ - i f_{-\kappa}^- \right)$$

$$f_\kappa^R = \frac{1}{\sqrt{2}} \left(f_\kappa^+ + i f_{-\kappa}^- \right), \qquad (A1)$$

corresponds to the radial wave functions for a left-handed and right-handed fermion respectively.

From Eqs. (13), (15) and $(f^+, f^-)^T = M(\hat{f}^+, \hat{f}^-)$ one gets

$$
\begin{aligned}
f_\kappa^+ &= i\sqrt{\varepsilon} \left(\hat{f}_\kappa^- - \hat{f}_\kappa^+ \right) \\
&= i\sqrt{\varepsilon} \frac{1}{x} \left[\frac{s - i\varepsilon}{\kappa} C_1^{(\kappa)} M_{\rho_+, s}(2i\varepsilon x^2) - C_1^{(\kappa)} M_{\rho_-, s}(2i\varepsilon x^2) \right],
\end{aligned}
$$
(A2)

$$
\begin{aligned}
f_{-\kappa}^- &= \sqrt{\varepsilon} \left(\hat{f}_{-\kappa}^- + \hat{f}_{-\kappa}^+ \right) \\
&= \sqrt{\varepsilon} \frac{1}{x} \left[\frac{s - i\varepsilon}{-\kappa} C_1^{(-\kappa)} M_{\rho_+, s}(2i\varepsilon x^2) + C_1^{(-\kappa)} M_{\rho_-, s}(2i\varepsilon x^2) \right],
\end{aligned}
$$
(A3)

where we used the condition $C_2 = 0$ as already mentioned in the main text for obtaining the phase shifts (17).

Now by imposing the condition $f_\kappa^R = 0$ and having in mind Eq. (16), together with the fact that $M_{\rho_+, s}$ and $M_{\rho_-, s}$ are

linearly independent, we obtain in the end the following relation

$$C_1^{(\kappa)} = C_1^{(-\kappa)}. \tag{A4}$$

Now calculating f_κ^L using Eq. (A4), we obtain in the end

$$f_\kappa^L = \sqrt{2} f_\kappa^+. \tag{A5}$$

The last equation tells us that by applying the partial wave analysis to the left-handed neutrino f_κ^L we will get the same phase shifts (17) as obtained by applying the partial wave analysis to the fermion spinor f_κ^+.

References

1 K. W. Ford and J. A. Wheeler, Ann. Phys. (Leipzig), **7**: 259 (1959)
2 C. Darwin, Proc. R. Soc. A, **249**: 180 (1959)
3 R. A. Matzner, J. Math. Phys. (N.Y.), **9**: 163 (1968)
4 P. A. Collins, R. Delbourgo, and R. M. Williams, J. Phys. A., **6**: 161 (1973)
5 W. G. Unruh, Phys. Rev. D, **14**: 3251 (1976)
6 N. G. Sanchez, Phys. Rev. D, **16**: 937 (1977); Phys. Rev. D, **18**: 1030 (1978)
7 T.-R. Zhang and C. DeWitt-Morette, Phys. Rev. Lett., **52**: 2313 (1984)
8 R. A. Matzner, C. DeWitte-Morette, B. Nelson, and T.-R. Zhang, Phys. Rev. D, **31**: 1869 (1985)
9 J. A. H. Futterman, F. A. Handler, R. A. Matzner, *Scattering from Black Holes* (Cambridge: Cambridge University Press, 1988)
10 A. B. Gaina, Sov. Phys. JETP, **69**: 13–16, (1989); Zh. Eksp. Teor. Fiz., **96**: 25–31 (1989)
11 A.B. Gaina, Sov. Phys. J., **31**: 544–548 (1989)
12 P. Anninos, C. DeWitt-Morette, R. A. Matzner, P. Yioutas, and T. R. Zhang, Phys. Rev. D, **46**: 4477 (1992)
13 N. Andersson, Phys. Rev. D, **52**: 1808 (1995)
14 A. Higuchi, Classical Quantum Gravity, **18**: L139 (2001); **19**: 599 (2002)
15 E. Jung, S. H. Kim, and D. K. Park, Phys. Lett. B, **602**: 105 (2004)
16 E. Jung and D. K. Park, Nucl. Phys. B, **717**: 272 (2005)
17 L. C. B. Crispino, S. Dolan, E. S. Oliveira, Phys. Rev. D, **79**: 064022 (2009)
18 D. Batic, N. G. Kelkar, and M. Nowakowski, Phys. Rev. D, **86**: 104060 (2012)
19 C. F. B. Macedo, L. C. S. Leite, E. S. Oliveira, S. R. Dolan, and L. C. B. Crispino, Phys. Rev. D, **88**: 064033 (2013)
20 K.-i. Kanai and Y. Nambu, Class. Quant. Grav., **30**: 175002 (2013)
21 C. L. Benone, E. S. de Oliveira, S. R. Dolan, and L. C. B. Crispino, Phys. Rev. D, **89**: 104053 (2014)
22 C. F. B. Macedo, L. C. B. Crispino, Phys. Rev. D, **90**: 064001 (2014)
23 A. Gubmann, Class. Quant. Grav., **34**: 065007 (2017)
24 B. Mashhoon, Phys. Rev. D, **7**: 2807–2814 (1973)
25 V. P. Frolov, A. A. Shoom, Phys. Rev. D, **86**: 024010 (2012)
26 R. Fabbri, Phys. Rev. D, **12**: 933–942 (1975)
27 T. Kobayashi, A. Tomimatsu, Phys. Rev. D, **82**: 084026 (2010)
28 R. A. Konoplya, A. Zhidenko, Phys. Rev. D, **87**: 024044 (2013)
29 L. C. B. Crispino, E. S. Oliveira, A. Higuchi, and G. E. A. Matsas, Phys. Rev. D, **75**: 104012 (2007)
30 L. C. B. Crispino, S. R. Dolan, and E. S. Oliveira, Phys. Rev. Lett., **102**: 231103 (2009)
31 L. C. B. Crispino, A. Higuchi, and E. S. Oliveira, Phys. Rev. D, **80**: 104026 (2009)
32 L. C. B. Crispino, S. R. Dolan, A. Higuchi, and E. S. de Oliveira, Phys. Rev. D, **90**: 064027 (2014)
33 C. V. Vishveshwara, Nature, **227**: 936–938 (1970)
34 P. J. Westervelt, Phys. Rev. D, **3**: 2319–2324 (1971)
35 P. C. Peters, Phys. Rev. D, **13**: 775–777 (1976)
36 F. A. Handler, R. A. Matzner, Phys. Rev. D, **22**: 2331–2348 (1980)
37 S. R. Dolan, Class. Quant. Grav., **25**: 235002 (2008)
38 S. R. Dolan, Phys. Rev. D, **77**: 044004 (2008)
39 S. Creek, O. Efthimiou, P. Kanti, and K. Tamvakis, Phys. Lett. B, **635**: 39 (2006)
40 F. Sorge, Class. Quant. Grav., **32**: 035007 (2015)
41 S. R. Das, G. Gibbons, and S. D. Mathur, Phys. Rev. Lett., **78**: 417 (1997)
42 W. M. Jin, Classical and Quantum Gravity, **15**(10): 3163 (1998)
43 C. Doran and A. Lasenby, Phys. Rev, D, **66**: 024006 (2002)
44 E. Jung, S. H. Kim, and D. K. Park, JHEP, **09**: 005 (2004)
45 H. Cho and Y. Lin, Classical and Quantum Gravity, **22**(5): 775 (2005)
46 S. Dolan, C. Doran, and A. Lasenby, Phys. Rev. D, **74**: 064005 (2006)
47 M. Rogatko and A. Szyplowska, Phys. Rev. D, **79**: 104005 (2009)
48 H. Huang, M. Jiang, J. Chen, Y. Wang, Gen Relativ Gravit, **47**: 8 (2015)
49 I. I. Cotăescu, C. Crucean, and C. A. Sporea, Eur. Phys. J. C, **76**: 102 (2016)
50 I.I. Cotăescu, C. Crucean, C.A. Sporea, Eur. Phys. J. C **76**:413 (2016)
51 H. Liao, J-H. Chen, P. Liao, and Y-J. Wang, Commun. Theor. Phys., **62**: 227–234 (2014)
52 A. Ghosh, P. Mitra, Phys. Rev. D, **50**: 7389–7393 (1994)
53 G. W. Gibbons, Commun. Math. Phys., **44**: 245 (1975)
54 V. Cardoso, C. F. B. Macedo, P. Pani, and V. Ferrari, J. Cosmol. Astropart. Phys., **1605**: 054 (2016)
55 A. De Rujula, S. L. Glashow and U. Sarid, Nucl. Phys. B, **333**: 173 (1990)
56 C. F. B. Macedo, P. Pani, V. Cardoso, and L. C. B. Crispino, Astrophys. J., **774**: 48 (2013)
57 Y. Fukuda et al (Super-Kamiokande collaboration), Phys. Rev. Lett., **81**: 1562 (1998)
58 Q.R. Ahmad et al (SNO collaboration), Phys. Rev. Lett., **89**: 011301 (2002)
59 E. Giusarma, M. Gerbino, O. Mena, S. Vagnozzi, S. Ho, and K. Freese, Phys. Rev. D, **94**: 083522 (2016)
60 B. Thaller. *The Dirac Equation*, (Berlin Heidelberg: Springer Verlag, 1992)
61 V. B. Berestetski, E. M. Lifshitz and L. P. Pitaevski. *Quantum Electrodynamics*, (Oxford: Pergamon Press, 1982)
62 I. I. Cotăescu, Mod. Phys. Lett. A, **13**: 2923 (1998)
63 I. I. Cotăescu, J. Phys. A Math. Gen., **33**: 1977 (2000)
64 D. R. Yennie, D. G. Ravenhall, and R. N. Wilson, Phys. Rev., **95**: 500 (1954)
65 I. D. Novikov, *Doctoral Disertation*: Sthernberg Astronomical Institute (1963)
66 C. W. Misner, K. S. Thorne, and J. A. Wheeler, *Gravitation* (San Francisco: Freeman & Co., 1971)
67 F. W. J. Olver, D. W. Lozier, R. F. Boisvert, and C. W. Clark, *NIST Handbook of Mathematical Functions* (Cambridge University Press, 2010)
68 I. I. Cotăescu, Phys. Rev. D ,**60**: 124006-010 (1999); Phys. Rev. D, **65**: 084008 (2002)
69 C. A. Sporea, Mod. Phys. Lett. A, **30**: 1550145 (2015)
70 I. I. Cotăescu, Rom. J. Phys., **52**: 895–940 (2007)
71 I. I. Cotăescu, Mod. Phys. Lett. A, **22**: 2493 (2007)
72 N. Arkani-Hamed, S. Dimopoulos, and G. Dvali, Phys. Lett. B, **429**: 263 (1998)